

MONITORING VEGETATION BIOMASS IN RIVER FLOODPLAINS USING IMAGING SPECTROSCOPY

L. Kooistra^{a,*}, M.D. Suarez Baranco^a, H. van Dobben^b, M.E. Schaepman^a

^a Wageningen University, Centre for Geo-information, Droevendaalsesteeg 3,
NL 6708 PB, Wageningen, The Netherlands

^b Alterra, Landscape Centre, Droevendaalsesteeg 3,
NL 6708 PB, Wageningen, The Netherlands

KEY WORDS: plant functional type, aboveground biomass, mixture tuned match filtering (MTMF), imaging spectroscopy

ABSTRACT:

For optimal management of river floodplains in the Netherlands monitoring of natural vegetation succession and hydrodynamic processes is essential. A key biophysical parameter to monitor floodplains is vegetation biomass. Not only because it influences the hydraulic resistance determining the discharge capacity of the floodplains, but also indicating species diversity and habitat heterogeneity in the floodplains. The objective of this study is to investigate the feasibility of mapping above-ground biomass and plant functional type distribution of heterogeneous canopies in river floodplains using imaging spectroscopy.

We establish linear predictive models between vegetation indices derived from airborne imaging spectrometer (HyMap) data and field measurements of biomass ($n = 21$). Image and field data were acquired during a field campaign in the summer of 2004 in the Millingerwaard, a river floodplain situated along the river Waal in the Netherlands. Results for broad-band and narrow-band derived VIs (e.g., NDVI, SAVI, WdVI and RSR) and a multivariate approach using PLS were compared using a cross-validation procedure to assess the prediction power of the regression models. Results showed that regression models could be improved when differences in vegetation structure were taken into account. Therefore, regression models were developed for individual plant functional types (grassland, mixed herbaceous, shrub and softwood forest). Vegetation biomass maps for the Millingerwaard were prepared in two steps. First a classification of plant functional types was made using mixture tuned match filtering (MTMF). In a second step, the best regression models were inverted and used to map the spatial distribution of the vegetation biomass. The results demonstrate the necessity to use a PFT based approach for biomass assessment, improving the quality of the prediction significantly over conventional approaches.

1. INTRODUCTION

River floodplains are dynamic systems and in Western-Europe they are often determined to combine different functions, such as flood protection, nature development, recreation, agriculture and extraction of sand, clay and gravel (Middelkoop *et al.*, 2001). For optimal management of these river systems monitoring of vegetation succession is an essential requirement. On the hand it gives insight in the inherent quality of the floodplain in terms of e.g., biodiversity. On the other hand, the influence of vegetation on the hydraulic resistance of the floodplains is used for modelling current and future discharge capacities of the river system. For example in the Netherlands, river managers require information on the spatial distribution of vegetation biomass in river floodplains to decide for which locations increased flood risks occur.

Future development of vegetation succession is assessed by comparing scenarios from ecological process models. Recent advances in remote sensing have shown that imaging spectroscopy can be applied for quantitative retrieval of relevant vegetation variables (e.g., LAI, biomass, vegetation structure) that are required for model initialization and calibration (Turner *et al.*, 2004) but also for monitoring of the actual status of the floodplain.

Vegetation biomass mapping in river floodplains is complicated due to the significant spatial variability of vegetation

composition. For modelling applications, functional classifications have been developed to simplify the floristic complexity (Woodward and Cramer, 1996). This means that classes of plant functional types (PFT) are composed of species with a similar effect on one or several ecosystem functions (e.g., primary productivity, nutrient cycling). To improve mapping of biophysical variables it has been suggested to derive land cover specific relationships using land cover maps (Cohen *et al.*, 2003). This suggestion could also be adopted for biomass mapping by stratifying the area for specific plant functional types.

The objective of this study is to investigate the feasibility of mapping above-ground biomass of heterogeneous canopies in river floodplains using imaging spectroscopy using a PFT based approach. The suitability of univariate regression models based on vegetation indices is compared to the use of a multivariate regression model using PLS. In addition, the use of plant functional type specific relations is evaluated.

2. MATERIAL AND METHODS

2.1 Study area

The Millingerwaard floodplain is a heterogeneous natural area along the river Waal in the Netherlands. As part of the Gelderse Poort nature reserve, the floodplain is a nature rehabilitation area, meaning that for some time now areas have been taken out of agricultural production and are allowed to undergo natural

* Corresponding author: email: Lammert.Kooistra@wur.nl

succession. This has resulted in a heterogeneous landscape with river dunes along the river (PFT22), a large softwood forest in the eastern part along the winterdike (PFT4) and in the intermediate area a mosaic pattern of different succession stages (PFT1, PFT21, PFT22 and PFT3) (see table 1). Nature management (e.g., grazing) within the floodplain is aiming at improvement of biodiversity. However, also measures for reduction of the hydraulic resistance of the vegetation (e.g., harvesting of softwood forest) have been carried out.

Plant functional type	height (m)	main species
PFT1: grazed grassland	0 - 0.4	<i>Trifolium rep.</i> , <i>Potentilla rept.</i> , <i>Cynodon dactylon</i>
PFT21: Mixed herbaceous – Echio Melilotetum	0.8 - 1.3	<i>Rubus caesius</i> , <i>Urtica dioica</i>
PFT22: : Mixed herbaceous – Bromo Inermis	0.4 - 1	<i>Calamagrostis epigejos</i>
PFT3: shrubs	0.8 - 4	<i>Sambucus nigra</i> , <i>Cratageus monogyna</i>
PFT4: softwood forest	> 2	<i>Salix alba</i>

Table 1. Main plant functional types for vegetation in floodplain Millingerwaard along the river Waal in the Netherlands

2.2 Spectrometer data

HyMap images for the Millingerwaard were acquired on July 28, 2004 in 126 spectral bands ranging from 400 to 2500 nm (bandwidth 15 - 20 nm). The data were processed to surface reflectance by partially compensating for adjacency effects and directional effects using the model combination PARGE/ATCOR-4 (Richter and Schläpfer, 2002). The spatial resolution of the images is 5 m. Ground measurements include top-of-canopy reflectance measurements as well as leaf optical properties measurements at all ground plots as well as several reflectance measurements of calibration surfaces using an ASD FieldSpec instrument (Kooistra *et al.*, 2005). A mask was applied to select the vegetated areas within the floodplain, based on pixels with an NDVI > 0.2 and a maximum reflectance at the wavelength of 665 nm (band 13) of 7.4 %.

2.3 Field sampling

We selected 21 sampling plots measuring 2x2 m, covering the plant functional types grassland (PFT1) and mixed herbaceous vegetation (PFT21 and PFT22). Vegetation biomass was sampled in three subplots (0.5x0.5 m) with a homogeneous vegetation cover located at three of the corners of each main plot. Biomass was clipped at 0.5 cm above the ground level and stored in paper bags. The collected material was air-dried, first for 5 days at room temperature in open bags, and subsequently for 24 h at 70°C, and weighed. For every sampling plot a detailed vegetation description was made according to the method of Braun-Blanquet (1951). Abundance per species was estimated optically as percentage soil covered by living biomass in vertical projection, and scored in a nine-point scale. The coordinates of the central location of each ground plot was determined using a differential global positioning system.

2.4 Biomass regression models

The DGPS measured locations of the sampling plots were overlaid on the HyMap image and reflectance spectra were extracted for single pixels that coincided with the plots. Various

vegetation indices were calculated and tested as predictor for vegetation biomass. As earlier studies often show a saturation effect for higher biomass values (e.g., Wylie *et al.*, 2002), both linear and exponential regression models were tested. A cross-section of frequently used vegetation indices (VIs) was assessed in this study. This included the traditional NDVI and Ratio index (both SR and RSR), the soil-correcting WDI and SAVI, the atmosphere-correcting index GEMI, the EVI as used for MODIS data and the MTCI as used for MERIS data. In addition, several narrow band indices were tested PVI, TVI, MCARI and VOG. An overview of most of the indices can be found in Broge and Leblanc (2001).

Results of the univariate regression approach using VIs were compared with a multivariate regression approach using partial least squares (PLS) regression. Because of the low number of available samples, we used the leave-one-out (LOO) cross-validation procedure to validate the regression models. Because the predicted samples are not the same as the samples used to build the model, the RMSE of cross-validation (RMSECV) is a good indicator of the accuracy of the model in predicting unknown samples. In addition, the RMSECV was used to select the optimal number of latent variables for the PLS model.

2.5 Mapping spatial distribution of biomass

Vegetation biomass maps for the Millingerwaard were prepared in two steps. First a classification of plant functional types was made using mixture tuned match filtering (MTMF). Next, the best regression models were inverted and used to map the spatial distribution of the vegetation biomass.

A minimum noise fraction (MNF) was performed to reduce the noise level and to optimise the classification. After visual inspection the first 8 new composite bands were selected as inputs for the classification. Earlier studies have shown that MTMF can give good classification results for heterogeneous vegetation cover (Williams and Hunt, 2002; Glenn *et al.*, 2005). MTMF is a unmixing algorithm that is capable of determining the abundance of different end-members within a pixel. End-member spectra for PFT1, PFT21 and PFT22 (Table 1) in the Millingerwaard were collected from the DGPS measured locations. End-member spectra for PFT3 (shrubs), PFT4 (forest), agricultural crops and soil were collected by manual selection of regions of interest. This was supported by field knowledge and aerial photographs. The MTMF algorithm produces a matched filter value for every end-member for every pixel of the masked HyMap image. The final biomass map was constructed by combining the matched filter values with the inverted regression models for the investigated PFTs.

3. RESULTS AND DISCUSSION

3.1 Biomass statistics per plant functional type

The plant functional type for every sampling location was derived from the vegetation descriptions based on height and species composition. The relationship between the vegetation species was explored using Detrended Correspondence Analysis (DCA) based on the software program Canoco (ter Braak and Smilauer, 2002). In the resulting DCA-plot (Figure 1) the species variation for the sampling plots is presented. Variation on the first axis is explained by a dry-wet gradient from the levees (high, sandy) to lower, clay-rich soils, perpendicular to the river. The second axis represents (natural) management with high values for grazed plots. Based on the

position of the sampling locations in the DCA-plot, a clustering of samples per PFT was identified (Figure 1). In 2004, no sampling plots were located in shrubs and softwood forest, so these PFTs are not shown in the DCA-plot. Table 2 summarises the biomass statistics for the measured PFTs. The biomass range for grazed grassland is clearly lower than the herbaceous vegetation types. PFT21 dominated by *Rubus caesius* shows both higher mean and maximum values than PFT22 that occurs on the higher located levees.

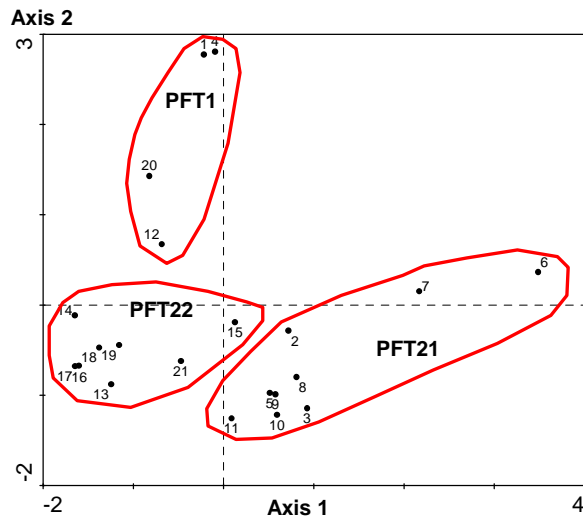


Figure 1. DCA plot of the vegetation species described for the 21 sampling plots in the Millingerwaard.

Plant functional type	n	biomass (ton/ha)			
		mean	stdev	min	max
PFT1: grazed grassland	4	1,68	0,61	1,27	2,59
PFT21: Mixed herbaceous – Echio Melilotetum	8	7,32	1,73	5,81	11,6
PFT22: Mixed herbaceous – Bromo Inermis	9	4,49	1,30	2,42	6,46

Table 2. Summary statistics for measured biomass in 21 plots for the identified plant functional types in the Millingerwaard

3.2 Regression of biomass and spectral reflectance

A preliminary analysis of the relationship between the investigated VIs and vegetation biomass revealed PFT specific behaviour (Figure 2). The combined set of herbaceous vegetation plots for PFT21 and PFT22 shows a clear relation between SAVI and measured biomass. However, figure 2 shows that grazing influences the relation between reflectance and biomass: the grazed plots (PFT1) appear to have a higher LAI at a given biomass compared to the ones not grazed. For this study, the plots of PFT1 were excluded from our analysis because their low number prevented a separate calibration.

Plots of the (absolute value of the) correlation coefficient provide more insight in the relationship between the HyMap derived reflectance and the measured biomass (Figure 3). The largest absolute value for the correlation coefficient was found at 1023 nm, however the whole NIR region from 770 – 1130 nm shows values around the maximum. Correlation for the visible bands (440-695 nm) was negative, for near-infrared (710-1340 nm) positive, and negative for the short-wave infrared.

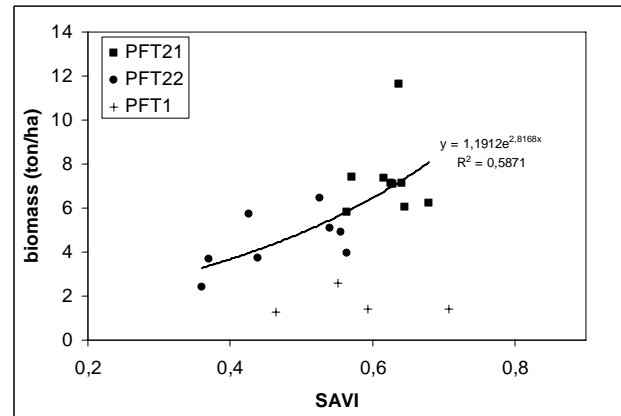


Figure 2. Relation between SAVI derived from HyMap reflectance spectra and biomass for all measured plots (n=21)

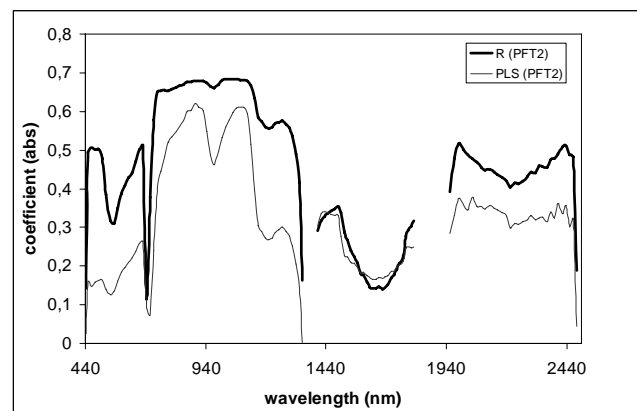


Figure 3. Absolute value of correlation coefficients and PLS regression coefficient (divided by factor 100) relating HyMap reflectance to biomass for herbaceous vegetation (PFT2)

For the combined set of mixed herbaceous sampling plots (PFT21 and PFT22), various vegetation indices were tested as predictor for biomass. Best results with only small differences in R^2 and RMSECV were obtained for SAVI, WdVI and GEMI using exponential relationships (Table 3). From these results can be deduced that although vegetation coverage for large parts of the area is high, the background reflectance of the soil is also an important component to consider. Although other studies showed good results for NDVI in grassland (Wylie *et al.*, 2002), relationships with NDVI in this study resulted in higher cross-validation errors. Also, the use of hyperspectral based indices (e.g., MCARI, Vog) resulted in higher cross-validation errors (1.84 and 1.74, respectively). As could be expected (Figure 2), including the grassland samples in the regression analysis, resulted in a significant reduction of the prediction capability.

Vegetation index	R^2	RMSECV
NDVI	0,498	1,79
SAVI	0,588	1,66
WdVI	0,583	1,68
GEMI	0,587	1,65
PLS (2 factors)	0,517	1,58

Table 3. Results of (selection of) investigated vegetation indices and PLS for estimation of biomass of mixed herbaceous vegetation (PFT2)

Finally, PLS was used to investigate the multivariate relation between biomass and HyMap reflectance. Compared to the three best VIs this resulted in an improved cross-validation error but a lower R^2 . Due to its linear character PLS is less capable of predicting the higher values of the biomass range. Investigation of the PLS regression coefficient shows that clear maxima can be identified around 895 and 1099 nm. Possibly, this could be related with the slopes of the water absorption features around 970 and 1200 nm.

3.3 Spatial distribution of biomass

The following step in this study was to predict the value of the biomass on the basis of the HyMap reflectance values. As PFT specific relations for mixed herbaceous vegetation have been derived, first the coverage of this PFT in the Millingerwaard needs to be determined. From the MTMF classification results, clear differences can be observed in the spatial coverage of grazed grassland (PFT1) and mixed herbaceous vegetation (PFT21 and PFT22) in the Millingerwaard (Figure 4). Although grazed grassland occurs in several areas of the floodplain (Figure 4A), a clear hotspot can be observed in triangular area in the north of the floodplain which is a former agricultural field under grazing management. In the central area of the floodplain, smaller grazing areas and paths which is used by the cattle can be identified. The coverage of PFT21, which is dominated by *Rubus caesius*, is mainly concentrated in the central area of the floodplain. The coverage of PFT22, is spread over a large part of the floodplain, but excludes the *Rubus caesius* dominated area of PFT21. The coverage of PFT22 along the river on the levee is expected. As main understory of the softwood forest, it also covers a large part of the south-east area of the floodplain where the softwood forest is located.

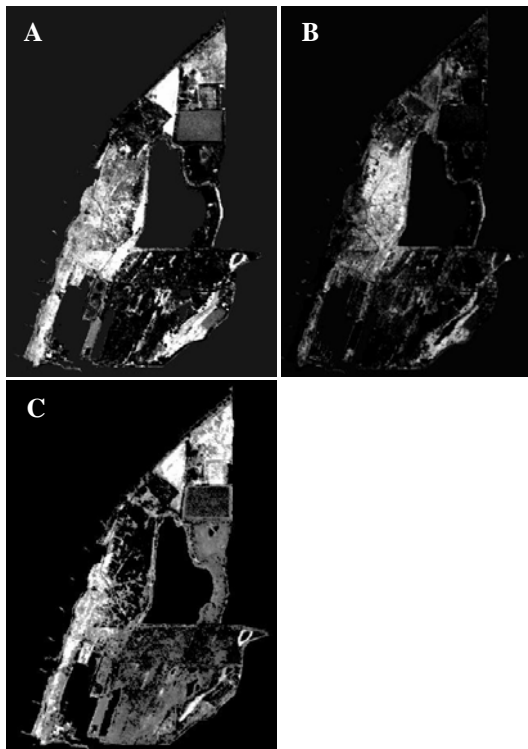


Figure 4. Results of MTMF classification: matched filter values are presented for (A) PFT1, (B) PFT21 and (C) PFT22 (see Table 1 for description of PFTs).

Figure 4C also shows the mixing of PFT1 and PFT22 in the former agricultural field to the North. Although a certain level of mixing can be expected, the coverage of PFT22 seems to be overestimated. Further analysis is required to assess the classification accuracy in a quantitative manner.

Based on the coverage of the mixed herbaceous PFT (Figure 4B and 4C), the spatial distribution of biomass for this PFT was calculated. The biomass map of herbaceous vegetation was computed through inversion of the SAVI based exponential regression model (Figure 5) proportionally to the coverage of PFT21 and PFT22. In the central part of the floodplain, the spatial distribution of mixed herbaceous biomass shows increasing values perpendicular to the river. On the levee along the river, vegetation biomass is relatively low; further from the river vegetation coverage increases and also vegetation biomass increases. In the softwood forest, relatively lower biomass values for herbaceous vegetation are estimated due to the mixed vegetation in the pixels. Due to uncertainty in the classification, the agricultural field in North-Eastern part of the floodplain shows estimated biomass values, while this area is covered by maize.

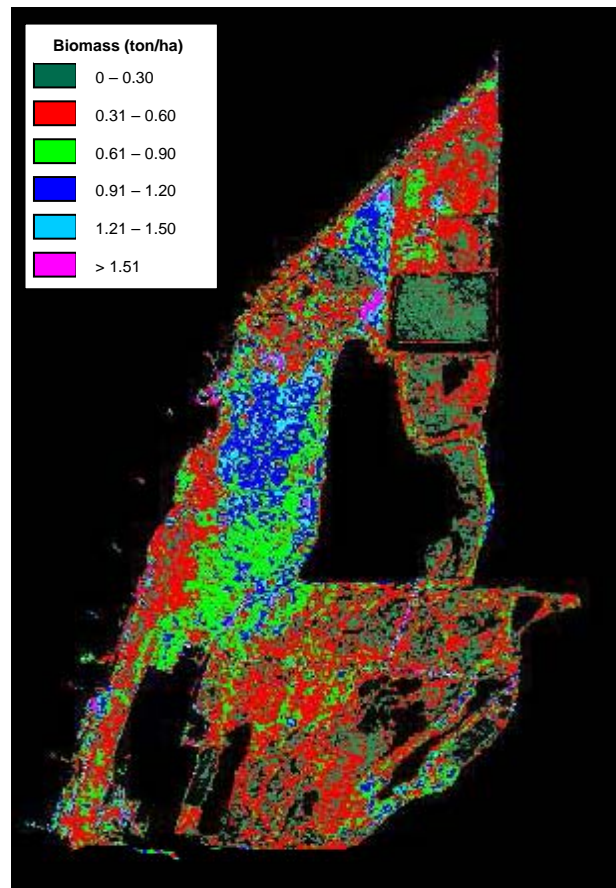


Figure 5. Above-ground biomass (ton/ha) of herbaceous vegetation (PFT2) predicted using SAVI vegetation index for the Millingerwaard

4. CONCLUSIONS

We explore the possibility to assess vegetation biomass in a heterogeneous river floodplain using imaging spectroscopy. The results indicate that biomass can be estimated with a reasonable accuracy using both VI's-based approaches and PLS regression. However, we found that the quality of these relations are significantly dependent on a pre-classification of the imaging spectrometer data into plant functional types. For example in the Millingerwaard, nature management through grazing had an important influence on the relation between vegetation reflectance and biomass. Based on a first qualitative evaluation, we can conclude that by applying mixture tuned match filtering (MTMF), a good characterization of the spatial distribution of PFTs within the floodplain could be made.

In future work, we will use physical based modelling for the retrieval of biophysical parameters in dependency of PFT estimates.

ACKNOWLEDGEMENTS

The authors wish to acknowledge the Belgian Science Policy Office for providing the HyMap data-set and Staatsbosbeheer for their permission to access the Millingerwaard test area.

REFERENCES

Broge, N.H., and Leblanc, E., 2001. Comparing prediction power and stability of broadband and hyperspectral vegetation indices for estimation of green leaf area index and canopy chlorophyll density. *Remote Sensing of Environment*, 76(2), pp. 156-172.

Cohen, W.B., Maersperger, T.K., Gower, S.T., and Turner, D.P., 2003. An improved strategy for regression of biophysical variables and Landsat ETM+ data. *Remote Sensing of Environment*, 84, pp. 561-571.

Glenn, N.F., Mundt, J.T., Weber, K.T., Prather, T.S., Lass, L.W., and Pettingill, J., 2005. Hyperspectral data processing for repeat detection of small infestations of leafy spurge. *Remote Sensing of Environment*, 95, pp. 399-412.

Kooistra, L., Clevers, J., Schaepman, M., van Dobben, H., Sykora, K., Holtland, J., Batelaan, O., Debruyne, W., Bogaert, J., Schmidt, A., Clement, J., Bloemmen, M., Mucher, C.A., van den Hoof, C., de Bruin, S., Stuver, J., Zurita, R., Malenovsky, Z., Wenting, P., Mengesha, T., van Oort, P.A.J., Liras Laita, E., Wamelink, W., Schaepman-Strub, G., Hung, L.Q., Verbeiren, B., Bertels, L., & Sterckx, S., 2005. Linking Biochemical and Biophysical Variables Derived from Imaging Spectrometers to Ecological Models - The HyEco'04 Group Shoot. In 4th Workshop on Imaging Spectroscopy (eds B. Zagajewski, M. Sobczak & W. Prochnicki), Vol. 1, pp. 61. EARSeL, Warsaw.

Middelkoop, H., Daamen, K., Gellens, D., Grabs, W., Kwadijk, J.C.J., Lang, H., Parmet, B.W.A.H., Schadler, B., Schulla, J., and Wilke, K., 2001. Impact of climate change on hydrological regimes and water resource management in the Rhine basin. *Climate Change*, 49, pp. 105-128.

Richter, R., and Schläpfer, D., 2002. Geo-atmospheric processing of wide FOV airborne imaging spectrometry data. In Proceedings of SPIE - The International Society for Optical Engineering, Vol. 4545, pp. 264.

Ter Braak, C. J. F., and Smilauer, P., 2002. Canoco reference manual and CanoDraw for Windows user's guide: software for canonical community ordination (version 4.5). Microcomputer Power, Ithaca, New York, USA.

Turner, D.P., Ollinger, S.V., and all, J.S., 2004. Integrating remote sensing and ecosystem process models for landscape- to regional-scale analysis of the carbon cycle. *BioScience*, 54, pp. 573-585.

Wylie, B.K., Meyer, D.J., Tieszen, L.L., and Mannel, S., 2002. Satellite mapping of surface biophysical parameters at the biome scale over the North American grasslands. A case study. *Remote Sensing of Environment*, 79, pp. 266-278.

Williams, A.E.P. and Hunt, E.R., 2002. Estimation of leafy spurge cover from hyperspectral imagery using mixture tuned matched filtering. *Remote Sensing of Environment*, 57, pp. 106-112.

Woodward, F.I., and Cramer, W., 1996. Plant functional types and climate changes: introduction. *Journal of Vegetation Science*, 7, pp. 306-308.